

An Experimental Study on Rayleigh Scattering

Rayleigh Şaçılma Üzerine Deneysel Bir Çalışma

Abstract

The Rayleigh scattering cross-sections were determined in the region of $22 \leq Z \leq 82$ at 126° using an energy dispersive X-ray fluorescence spectrometer at 59.5 keV energy and a Si(Li) detector. This paper presents and discusses the results of this study. The predictions of several form factor theories were compared with experimental Rayleigh scattering differential cross-sections

Keywords: Rayleigh scattering, Differential cross section, X-ray fluorescence spectrometer

Öz

Bu çalışmada, Rayleigh saçılma diferansiyel tesir kesitleri enerji ayrımlı X-ışını flöresans spektrometreyle $22 \leq Z \leq 82$ bölgesinde 126° lik saçılma açısında ölçüldü. Deneyde 59.5 keV enerjili fotonlar ve bir Si(Li) dedektörü kullanıldı. Sonuçlar bu makalede sunuldu ve tartışıldı. Deneysel Rayleigh saçılma diferansiyel tesir kesitleri farklı form faktör teorilerinin sonuçlarıyla karşılaştırıldı.

Anahtar Kelimeler: Rayleigh saçılma, Diferansiyel tesir kesiti, X-ışını flöresans spektrometre

Salih Z. ERZENEÖĞLU 
Atatürk University, Department of Physics,
Faculty of Sciences, Erzurum, Turkey



Corresponding Author/ Sorumlu Yazar:
Salih Z. ERZENEÖĞLU
E-mail: salih@atauni.edu.tr

Received/ Geliş Tarihi 02.05.2024
Accepted/Kabul Tarihi 04.06.2024
Publication Date/
Yayın Tarihi 27.06.2024

Cite this article

Erzeneoglu, S. Z. (2024) An Experimental Study on Rayleigh Scattering. *Journal of Anatolian Physics and Astronomy*, 3(1), 1-6.



Content of this journal is licensed under a Creative Commons Attribution-Noncommercial 4.0 International License.

Introduction

Rayleigh scattering studies play a major role in fundamental atomic-physics research. For this reason, there has been much research in the literature. For the liver, kidney, muscle, and fat, Böke (2014) calculated coherent and incoherent scattering, photoelectric cross-sections, and linear attenuation coefficients. Thulasi et al. (2021) experimentally calculated the angle integrated total scattering cross sections of a few rare earth oxides for 59.54 keV gamma rays in the angular ranges of 0-40, 0-60, 0-80, and 0-100. They examined how the effective atomic number of the chosen compounds varied in relation to the angle-integrated coherent scattering cross-section. Angle-integrated coherent scattering cross-sections of a few components at modest momentum transfers throughout four angular ranges were published by (Vinaykumar & Umesh, 2016). The coherent (Rayleigh) to incoherent (Compton) scattering cross-section ratio of elements in the range $6 \leq Z \leq 82$ was experimentally established for 145 keV incident gamma photons by Singh et al. (2013). They were found to be in agreement with theoretical predictions based on the non-relativistic form factor, relativistic form factor, modified form factor, and S-matrix theory, which correspond to 4.939, 6.704, and 8.264 \AA^{-1} photon momentum transfer. At an energy of 59.54 keV, Thanh et al. (2020) used six well-known techniques to obtain experimental data of the Rayleigh to Compton scattering ratios depending on the effective atomic number of the 15 powder samples in the range $10 < Z < 30$. They fitted the Rayleigh peak using a Gaussian function using Root software and the Compton peak using a Voigt function using a new fitting process with the least squares method. Utilizing a Ge(Li) detector, İçelli and Erzeneoğlu (2002) determined differential cross-sections for coherent and Compton scattering of 59.5 keV gamma-rays at scattering 55° and 115° . Theoretical coherent and Compton scattering differential cross-sections were measured by interpolating atomic form factors and incoherent scattering functions corresponding to 2.216 and 4.048 \AA^{-1} photon momentum transfer. Rayleigh scattering cross section measurements for 39.5 keV (Sm-K α_2), 40.1 keV (Sm-K α_1), and 45.4 keV (Sm-K $\beta_{1,3}$) X-ray photons in 35 elements with $26 \leq Z \leq 83$ at a backward angle of 139° have been reported by Upmanyu et al. (2017). They carried out scattering experiments using a secondary photon source made up of a samarium (62Sm) target energized by 59.54 keV gamma-rays from the Am-241 radioactive source in a reflection-mode geometrical setup. To highlight the necessity of updating publicly accessible databases to incorporate the current atomic form factor tabulations, which allows the determination of a compound's linear differential scattering coefficient from a weighted sum of its elemental components. Tartari et al. (2005) have provided new small angle coherent scattering data. These data take into account the impact of the large-scale sample structure arrangement in addition to the molecular interference effect. Volotka et al. (2016) study theorize the Rayleigh scattering of X-rays by highly charged ions with numerous electrons. Beyond the independent-particle approximation (IPA), which is typically used to describe Rayleigh scattering, researchers have investigated many electron effects. Del Lama et al. (2015) have employed the Rayleigh to Compton scattering ratio (R/C) as a trustworthy quantitative technique for materials analysis, particularly biological ones. Their goal was to apply the R/C approach to determine which phantom was best suited to simulate biological tissues while taking into account two distinct experimental scenarios: scattering and attenuation. In the present study, Rayleigh scattering cross sections were reported for 14 elements.

Theoretical Basis

The differential cross-section for Rayleigh scattering of γ -rays by a target atom is obtained using the equation (Kane et al., 1983)

$$\frac{n}{n^{Al}} = \frac{T}{T^{Al}} \frac{N}{N^{Al}} \frac{\varepsilon}{\varepsilon^c} \left[\frac{d\sigma_{Al}}{d\Omega} \right]^{-1} \frac{d\sigma}{d\Omega} \quad (1)$$

where n is the number of photons Rayleigh scattered, n^{Al} is the number of photons Compton scattered from Al, T^{Al} and T are, respectively, the transmission factors for Al at the Compton energy and for 59.5 keV energy with the target, N^{Al} and N are the number of scattering atoms in Al and the scatterer, ε^c and ε are, respectively, the detector photopeak efficiencies for Compton and Rayleigh scattered γ -rays,

$$\frac{d\sigma_{Al}}{d\Omega} = \frac{d\sigma^{KN}}{d\Omega} S(x, Z) \quad (2)$$

is the Compton scattering cross-section for the aluminum, $d\sigma^{KN}/d\Omega$ is the Klein–Nishina cross-section per electron,

$S(x, Z)$ is the incoherent scattering function, x is the photon momentum transfer [$x = \sin(\theta/2)/\lambda$] \AA^{-1} , θ is the angle of scattering, λ is the wavelength of the incident radiation in Angstrom, Z is the atomic number of the scattering atom.

The theoretical Rayleigh scattering differential cross-section is calculated by using

$$\frac{d\sigma}{d\Omega} = \frac{1}{2} r_e^2 (1 + \cos^2\theta) [F(x, Z)]^2 \quad (3)$$

where r_e is the classical electron radius ($2.8179380 \times 10^{-15} \text{ m}$), $F(x, Z)$ is the atomic form factor.

Experimental Basis

The experimental setup used is given in Figure. 1. In this study, we used a point source of Am-241 with an intensity of 100 mCi which emits 59.5 keV gamma rays. The source was placed in lead blocks to collimate rays. We used a Si(Li) detector having 4 mm in active diameter and 3 mm in sensitive crystal depth. The resolution of the detector was 160 eV at 5.9 keV energy. Measurements were taken under the same experimental conditions for 10800 s. The spectra were recorded using a 1024 channel analyser. To obtain the net pulse height spectra of the scattered γ -rays, a background spectrum without the scatterer was stripped from the spectrum acquired for an equal period of time under experimental conditions. High-purity elemental powders of Ti, Ni, Zn, Se, Mo, Ru, Yb, Gd, Dy, W, and Pb (purity > 99.9%), and Cd, Sn, and Te (purity > 99.5%) were used as scatterers. The thicknesses of the powder elements ranged from 0.018 to 0.050 g/cm^2 . The target detector and target source distances were set to 5 cm, and the targets had an area of $25\pi \text{ mm}^2$. The scattering angle was 126° during the experiment. Particle size correction was performed using the following equation:

$$P = \frac{1 - \exp(-\mu d)}{\mu d} \quad (4)$$

where μ is the linear absorption coefficient (cm^{-1}) and d is the particle size (cm).

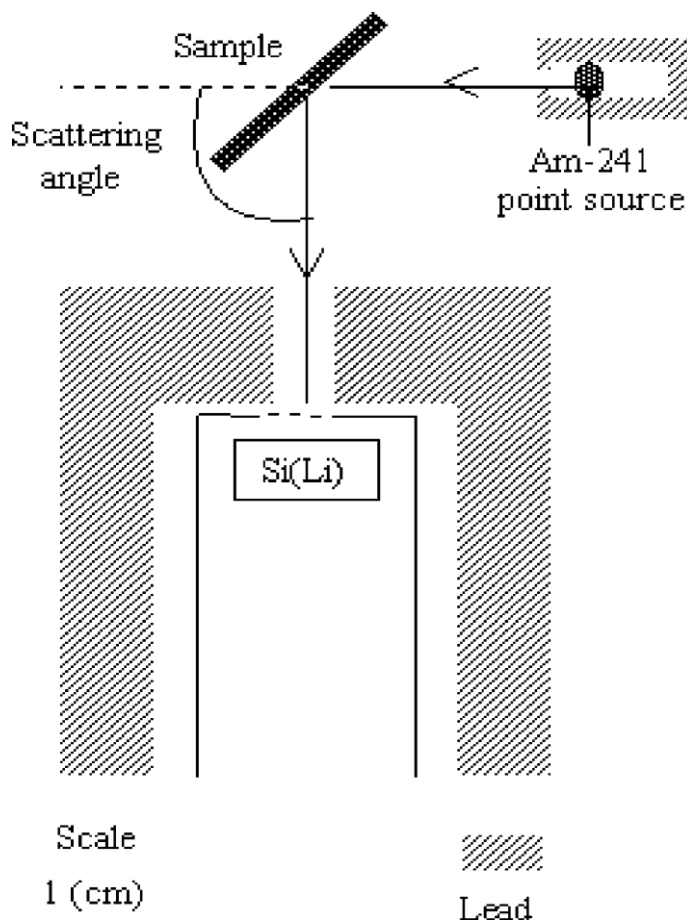


Figure 1. The experimental setup

Results and Discussion

The purpose of this research is to measure the Rayleigh scattering differential cross-sections of various materials. Table 1 displays the differential cross-sectional results for Rayleigh scattering, both theoretically and experimentally. Additionally, Fig. 2 presents a graphical comparison of the experimental data with the predictions of the nonrelativistic (NRFF) (Hubbell et al., 1975), relativistic (RFF) (Hubbell & O/Verbo, 1979), and relativistic modified form factor (RMFF) (Schaupp et al., 1983) theories. Differential scattering cross sections systematically increase with increasing atomic number, as shown in Fig. 2. It might be said that Rayleigh scattering becomes more prevalent as the atomic number rises since there are more electrons that are tightly bonded to nuclei. The contribution of Rayleigh is minimal for small-Z targets. The experimental results corresponded well with the predictions for all three formalisms in this region. The present experimental results, however, are smaller than the predictions of the NRFF and RFF theories, but are in good agreement with those of the RMFF theory in the high-Z zone. Furthermore, the findings highlight the significance of relativistic effects for high-Z components. Furthermore, the validity range of the form factor approximation for the bound electron description of elastic photon scattering is constrained (Kissel et al., 1980). In the total-atom form factor, the K shell predominates at bigger angles for this energy. Since L and higher shells become more significant and the form factor at this energy more precisely predicts these higher shells, the agreement between the experiment and predictions improves at smaller angles. For high-Z elements, the experimental results deviate from the theory, confirming the importance of electron-binding effects in the measurements. The experiment for Dy and Yb showed the largest difference between the predictions of the form factor approximation. This is because the K edges of these elements are closest to 59.9 keV (53.8 keV for Dy and 61.3 keV for Yb). Dispersion effects close to the K edges may be the cause of these anomalies. Previous studies have reported similar dispersion effects (Kissel et al., 1980), (Nayak et al., 1992). Less than 1.06% of the evaluations of the photopeak area were incorrect. The scattering angle precision is within $\pm 4\%$. The approximate estimate of inaccuracy in T was 2%.

Table 1. The experimental and theoretical differential cross sections (b/sr).

Element	Differential Cross section (b/sr)			
	Experimental	Theoretical		
		NRFF	RFF	RMFF
Ti	0.038	0.051	0.051	0.048
Ni	0.072	0.088	0.080	0.074
Zn	0.085	0.105	0.092	0.085
Se	0.110	0.149	0.128	0.117
Mo	0.258	0.299	0.280	0.251
Ru	0.315	0.350	0.338	0.303
Cd	0.433	0.463	0.478	0.425
Sn	0.522	0.525	0.556	0.493
Te	0.503	0.590	0.638	0.563
Gd	0.874	1.037	1.102	0.939
Dy	0.858	1.124	1.179	0.997
Yb	0.993	1.312	1.347	1.122
W	1.309	1.527	1.551	1.272
Pb	1.751	2.056	2.148	1.724

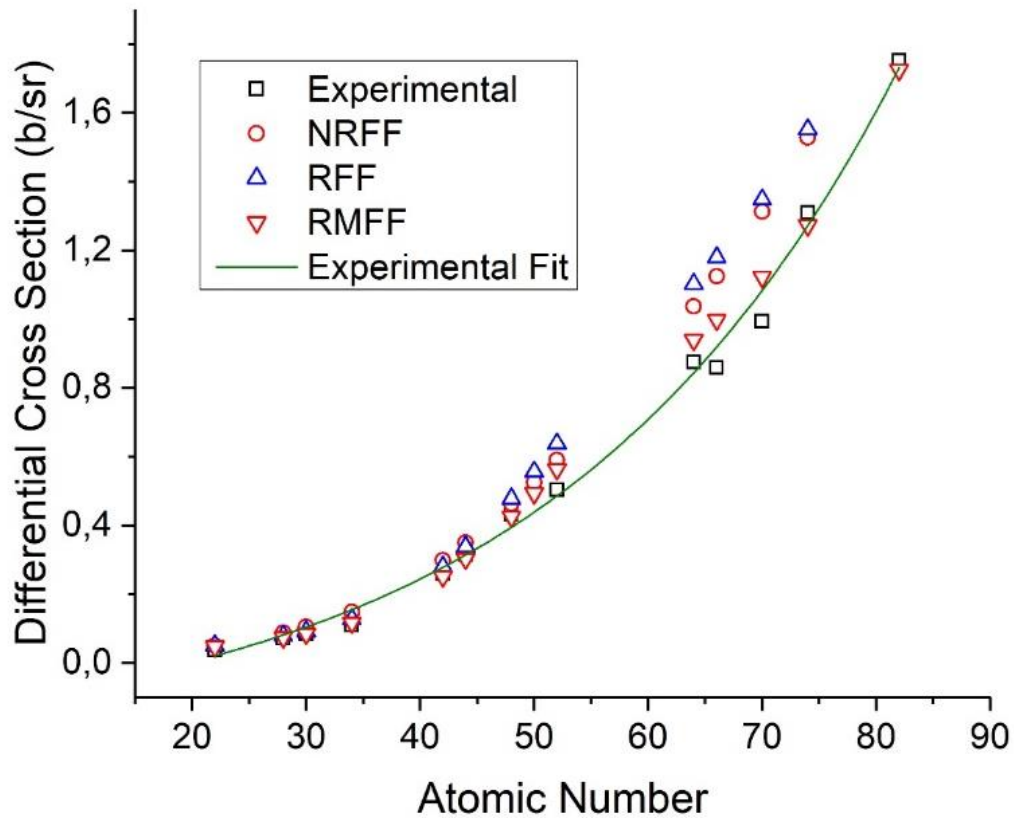


Figure 2. The differential cross section versus atomic number.

Conclusion

For photon energies of less than 2 MeV, elastic photon scattering is dominated by Rayleigh scattering and the contribution of bound atomic electrons to elastic photon scattering. Conversely, elastic scattering finds application in several experimental fields, including imaging, medical diagnostics, and material research. Among the mechanisms (photoeffect, scattering, and pair creation) principally responsible for attenuating thin beams of photons in matter is scattering, which plays a significant role in the energy range above the photoeffect L-edge but less than 10 MeV. I have provided precise values of the Rayleigh scattering differential cross sections for the elements Ti, Ni, Zn, Se, Mo, Ru, Cd, Sn, Te, Gd, Dy, Yb, W, and Pb in the current study. The current experimental study supports the superiority of the RMFF theory. In the future, similar research could be conducted using alternative approaches, energies, and scattering angles.

Peer-review: Externally peer-reviewed.

Conflict of Interest: The author has no conflicts of interest to declare.

Financial Disclosure: The author declared that this study has received no financial support.

Hakem Değerlendirmesi: Dış bağımsız.

Çıkar Çatışması: Yazar, çıkar çatışması olmadığını beyan etmiştir.

Finansal Destek: Yazar, bu çalışma için finansal destek almadığını beyan etmiştir.

References

- Böke, A. (2014). Linear attenuation coefficients of tissues from 1keV to 150keV. *Radiation Physics and Chemistry*, 102, 49–59. <https://doi.org/10.1016/j.radphyschem.2014.04.006>
- Del Lama, L., Soares, L., Antoniassi, M., & Poletti, M. (2015). Effective atomic numbers for materials of medical interest at low photon energy using the Rayleigh to Compton scattering ratio. *Nuclear Instruments and Methods in Physics Research. Section a, Accelerators, Spectrometers, Detectors and Associated Equipment/Nuclear Instruments & Methods in Physics Research. Section a, Accelerators, Spectrometers, Detectors and Associated Equipment*, 784, 597–601. <https://doi.org/10.1016/j.nima.2014.12.046>
- Hubbell, J. H., & O'Verbo, I. (1979). Relativistic atomic form factors and photon coherent scattering cross sections. *Journal of Physical and Chemical Reference Data*, 8(1), 69–106. <https://doi.org/10.1063/1.555593>
- Hubbell, J. H., Veigele, W. J., Briggs, E. A., Brown, R. T., Cromer, D. T., & Howerton, R. J. (1975). Atomic form factors, incoherent scattering functions, and photon scattering cross sections. *Journal of Physical and Chemical Reference Data*, 4(3), 471–538. <https://doi.org/10.1063/1.555523>
- İçelli, O., & Erzeneoğlu, S. (2002). Experimental study on ratios of coherent scattering to Compton scattering for elements with atomic numbers $26 \leq Z \leq 82$ in 59.5 keV for 55° and 115° . *Spectrochimica Acta. Part B, Atomic Spectroscopy*, 57(8), 1317–1323. [https://doi.org/10.1016/s0584-8547\(02\)00050-2](https://doi.org/10.1016/s0584-8547(02)00050-2)
- Kane, P. P., Mahajani, J., Basavaraju, G., & Priyadarsini, A. K. (1983). Scattering of 1.1732- and 1.3325-MeV gamma rays through small angles by carbon, aluminum, copper, tin, and lead. *Physical Review. A, General Physics*, 28(3), 1509–1516. <https://doi.org/10.1103/physreva.28.1509>
- Kissel, L., Pratt, R. H., & Roy, S. C. (1980). Rayleigh scattering by neutral atoms, 100 eV to 10 MeV. *Physical Review. A, General Physics*, 22(5), 1970–2004. <https://doi.org/10.1103/physreva.22.1970>
- Nayak, N. G., Siddappa, K., Balakrishna, K. M., & Lingappa, N. (1992). Coherent scattering of 59.5-keV γ rays by some medium and heavy elements. *Physical Review. A, Atomic, Molecular, and Optical Physics/Physical Review, a, Atomic, Molecular, and Optical Physics*, 45(7), 4490–4493. <https://doi.org/10.1103/physreva.45.4490>
- Schaupp, D., Schumacher, M., Smend, F., Rullhusen, P., & Hubbell, J. H. (1983). Small-Angle Rayleigh Scattering of Photons at High Energies: Tabulations of Relativistic HFS Modified Atomic Form Factors. *Journal of Physical and Chemical Reference Data*, 12(3), 467–512. <https://doi.org/10.1063/1.555690>
- Singh, M., Sharma, A., Singh, B., & Sandhu, B. (2013). An experimental study on cross-section ratio of coherent to incoherent scattering for 145 keV incident gamma photons. *Radiation Measurements*, 59, 30–36. <https://doi.org/10.1016/j.radmeas.2013.09.003>
- Tartari, A., Taibi, A., Bonifazzi, C., Gambaccini, M., & De Felici, M. (2005). Updating of x-ray coherent scattering cross-sections and their effects in microbeam and material analysis applications. *X-ray Spectrometry*, 34(5), 421–425. <https://doi.org/10.1002/xrs.847>
- Thanh, T. T., Minh, L. H., Cuong, N. Q. B., Chuong, H. D., Thong, N. D., Nguyen, V. H., Ho, P. L., Tai, C. T., & Van Tao, C. (2020). Study of different methods to estimate the Rayleigh to Compton scattering ratio and the effective atomic number ($10 < Z < 30$) using Si(Li) detector. *Nuclear Instruments and Methods in Physics Research. Section a, Accelerators, Spectrometers, Detectors and Associated Equipment/Nuclear Instruments & Methods in Physics Research. Section a, Accelerators, Spectrometers, Detectors and Associated Equipment*, 969, 163995. <https://doi.org/10.1016/j.nima.2020.163995>
- Thulasi, P. V., Joseph, A., Somashekarappa, H. M., & Kamat, V. A. (2021). Coherent Scattering Cross Sections of Some Rare Earth Compounds at Small Angles Below 10° for 59.54 KeV Gamma Rays. Social Science Research Network. <https://doi.org/10.2139/ssrn.3973501>
- Upmanyu, A., Singh, G., Duggal, H., Kainth, H., Bhalla, A., & Kumar, S. (2017). Measurement of large angle Rayleigh scattering cross sections for 39.5, 40.1 and 45.4 keV photons in elements with $26 \leq Z \leq 83$. *Applied Radiation and Isotopes*, 128, 125–131. <https://doi.org/10.1016/j.apradiso.2017.07.012>
- Vinaykumar, L., & Umesh, T. (2016). Small angle scattering of 59.54 keV photons by elemental samples in the atomic number region $13 \leq Z \leq 82$. *Journal of Radiation Research and Applied Sciences*, 9(1), 35–40. <https://doi.org/10.1016/j.jrras.2015.08.003>
- Volotka, A. V., Yerokhin, V. A., Surzhykov, A., Stöhlker, T., & Fritzsche, S. (2016). Many-electron effects on x-ray Rayleigh scattering by highly charged He-like ions. *Physical Review. A/Physical Review, A*, 93(2). <https://doi.org/10.1103/physreva.93.023418>